Leadership in Sustainable Infrastructure
Leadership en Infrastructures Durables

Vancouver, Canada
May 31 – June 3, 2017/ *Mai 31 – Juin 3, 2017*

INFLUENCE OF RELATIVE HUMIDITY ON CREEP AND RELAXATION BEHAVIOR OF CEMENT PASTE AT THE MICROSTRUCTURAL LEVEL

Frech Baronet, Jessy[1, 4] and Sorelli, Luca[2] and Chen, Zhao[3]
[1,2,3] Departement of Civil Engineering,Université Laval, Canada
[4] jessy.frech-baroent.1@ulaval.ca

Abstract: A recent survey showed that long term (20 to 50 years) delayed deflection on bridges was underestimated and exceeded by far the predicted values for design recommendations (Zdenek P Bažant, Hubler, & Yu, 2011). In order to evaluate this inaccurate prediction, the scientific community aims to develop new technique while studying the slow nature of creep (Jones & Grasley, 2011; Vandamme, 2008; Zhang, 2014). In recent studies, microindentation has revealed a powerful tool to assess the creep in cement paste in a short time period. The objective of this work is to study the duality between the creep and the relaxation phenomena, using simplified viscoelastoplastic models to quantify the moisture effect on the creep compliance function. The analysis elaborated throughout this paper is based on the hypothesis that the creep function follows a logarithmic law. The results show new insight to understand how the relative humidity affects the creep, the relaxation and the plasticity behaviour of cement paste.

1 INTRODUCTION

Deflection caused by long term creep phenomenon in concrete is of great interest to the civil engineering industry. A recent survey, published by Zdenek P Bažant et al. (2011), was performed on several bridges, monitored over a period of over 20 years. The results were thus: long term creep of concrete exceeds by far the prediction of several national codes. The sustainability of concrete structures is thus greatly affected, seen as an overdesign deformation, this kind of deflection can lead to undesired moment, which in its turn can lead to cracking, just as it occurred in the Koror-Babeldaob Bridge in 1996 (Zdenek P Bažant et al., 2011).

Creep is a phenomenon related to the microstructure of concrete. To account for the complexity of predicting long term creep, several theories have been proposed. Among them are: (i) the micro-diffusion of water in gel pores or adsorbed layers of calcium silicate hydrates (C-S-H) (Feldman, 1972); (ii) the sliding of C-S-H sheets (Miller, Bobko, Vandamme, & Ulm, 2008) and (iii) the gel compaction as a secondary consolidation process sliding of C-S-H sheets (Jennings, 2004).

It is generally assumed that at least two mechanisms are at stake to describe the short-term creep rate and the long-term creep rate. Short term creep is mainly due to water diffusion, while long term creep is due to the sliding of layered structures within the C-S-H gels (Benboudjema, Meftah, Sellier, Heinfling, & Torrenti, 2001; Vandamme, 2008). Moreover, among various parameters which affect concrete creep, the role of relative humidity (RH) is considered to be the most significant (Tamtsia & Beaudoin, 2000). However, despite the importance of RH, the available literature is limited, due to the time needed to reach moisture equilibrium for a sample of a few centimeters (Neville & Dilger, 1970). Indeed, several months are needed to reach hygral equilibrium. In 1958, Troxell, Raphael, and Davis (1958) performed a compressive test on concrete cylinders over a period of 30 years to study the influence of RH on long term creep. This test has since led to the development of alternative techniques, such as

microindentation, which allows assessing creep properties of cement paste, thus reducing significantly the time scale needed. Multiple authors (Nguyen, Alizadeh, Beaudoin, Pourbeik, & Raki, 2014; Zhang, 2014) have proved that microindentation tests correlate linearly with the macroscopic uniaxial compressive tests.

Although the simplicity of the microindentation technique is appealing to the scientific community, the measurement of indentation creep and relaxation are impeded by time-independent and instantaneous plastic deformations occurring during the test. Such deformation cannot be avoided and it is not trivial to separate plasticity from a viscoelastoplastic material. The aim of this work is to examine the link between the microindentation creep and the relaxation behaviour test, using an analytical viscoelastoplastic model based on creep compliance functions such as proposed by Vandamme, Tweedie, Constantinides, Ulm, and Van Vliet (2012).

2 MATERIAL AND METHOD

2.1 Basic of Microindentation

Microindentation is an innovative technique that has been successfully applied to the measure mechanical properties of cementitious materials (Constantinides, Ravi Chandran, Ulm, & Van Vliet, 2006; Ulm et al., 2007). The technique basically consists in applying a controlled force or a controlled displacement on the material, with a rigid conical diamond indenter, as sketched in Figure 1. The microindentation tests were carried out with the Anton-Paar instrument. A Berkovich indenter, which is a three-sided pyramid with an effective conical shape angle (α) of 70.3°, was employed.

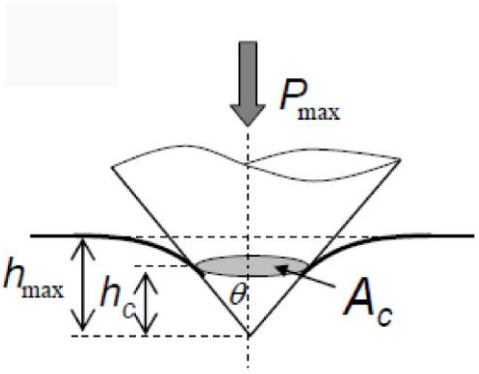

Figure 1: Schematic view of an indentation test with conical tip.

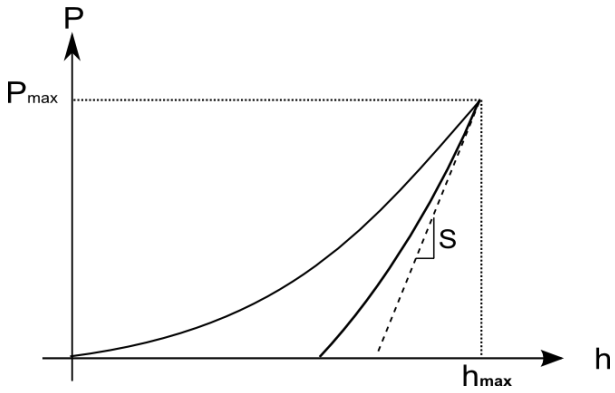

Figure 2: Mechanical response in term of load versus displacement.

To measure creep, a constant force (P_{max}) is maintained throughout the indentation test. The variation in displacement ($h\,(t)$) is measured to evaluate creep. Reciprocally, to measure relaxation, a constant displacement (h_{max}) is maintained and the variation of load ($P\,(t)$) is measured. The target value for P_{max} or h_{max} is reached with a linear progression. The time needed to reach the target P_{max} or h_{max} is the loading time τ_l. The time during which the target P_{max} or h_{max} is maintained is the loading time τ_h. The time at which point the tip is removed is the unloading time τ_u. The indentation parameters used are presented at Table 1.

From the load versus displacement curve ($P-h$) obtained (Figure 2), the mechanical properties can be extracted, such as the elastic modulus M and the hardness H. M is calculated with the equation [1.1], where the contact stiffness $S = dP/dh$ is the slope measured during the initial stage of the unloading curve, A_c is the projected area of contact and β is a coefficient that accounts for the slip on the indenter surface, which is about 1.034 for the Berkovich-type (Fischer-Cripps, 2009). H is calculated with the equation [1.2], where P_{max} is the maximum load reached during the test.

[1.1] $$M_0 = \frac{S\sqrt{\pi}}{2\beta\sqrt{A_c}}$$

[1.2] $$H = \frac{P_{max}}{A_c}$$

The contact area A_c is empirically calibrated on a sample of silica fuse of a certified indentation modulus, as follows (Fischer-Cripps, 2000):

[1. 3] $$A_c(h_c) = C_0h^2 + C_1h^1 + C_2h^{1/2} + C_3h^{1/4} + \cdots$$

where C_0 is 24.5 for an ideal conical shape of the indenter tip and the extra terms C_j are calibrated by the best fittings, and the experimental data over the range of interest is the penetration depth h_c.

2.2 Material for Microindentation Test

A smaller $3\ cm$ cube sample was extracted from the center of a cement paste $100\ mm\ x\ 200mm$ cylinder to perform the microindentation test. The sample's surface was carefully polished according to the criteria established by (Miller et al., 2008) in order to reduce the root mean square roughness (R_q) to less than 10 times the penetration depth ($R_q < \frac{h_{max}}{10}$). R_q is about $65\ nm$ as an average and was taken on three areas of $50\mu m\ x\ 50\ \mu m$. An Atomistic Force Microscope (AFM) was employed to verify the surface topography, as presented at Figure 3.

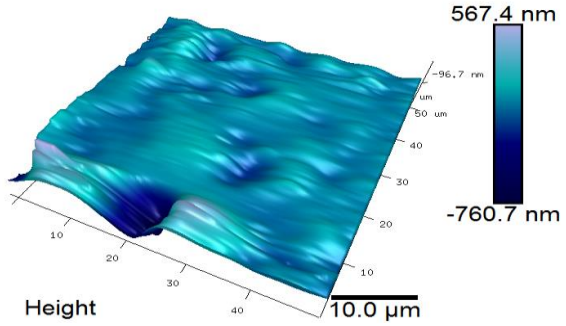

Figure 3: AFM surface topography on an area 50 x 50 μm.

Table 1: Microindentation testing parameters for the bulk cement paste

Parameters	Value
Grid size	10 x 10
Inter-distance	500 μm
P_{max}	8 N
h_{max}	40 μm
τ_l	5 s
τ_h	300 s
τ_u	5 s
RH (Salts)	33%, 55%, 75%, 85%

The microindenter was kept inside a hermetic enclosure, which consists of a closed circuit connected to an Erlenmeyer flask containing a saturated salt solution and a pump. The sample was cured at 33%, 55%, 75% and 85% of RH (see Table 1).

2.3 Creep of Concrete by Microindentation Technic Analysis: Microscopic scale.

The contact creep compliance $L(t)$ and contact relaxation modulus $M(t)$ characterize the time-dependent response. They are considered as material properties, since they do not depend neither on the geometry of the indenter nor on the value of P_{max} in force control or h_{max} in displacement control. However, time-dependant and instantaneous plastic deformation cannot be avoided below sharp probe (Vandamme et al., 2012). Therefore, the contact creep compliance is over-estimated and the relaxation modulus is under-estimated. However, Vandamme et al. (2012) have developed a method to separate the creep

from instantaneous plasticity response of a viscoelastoplastic material under contact loading. Furthermore,(Vandamme et al., 2012) have shown that in the case of relaxation, no further instantaneous plastic deformation occurs. On the other hand, in the context of creep, plasticity cannot be separated from viscoelastic behaviour.

2.3.1 Viscoelastoplastic analysis

The constitutive equations of an isotropic viscoelastic material are describe by the following convolution integrals (Christensen, 2012),

[1.4] $$\sigma(t) = \int_0^t E(t-\xi)\frac{\partial \varepsilon(\xi)}{\partial \xi} d\xi$$

[1.5] $$\varepsilon(t) = \int_0^t J(t-\xi)\frac{\partial \sigma(\xi)}{\partial \xi} d\xi$$

where $\sigma\,(t)$ and $\varepsilon\,(t)$ are the uniaxial stress and strain respectively. The function $E(t)$and $J(t)$ are the relaxation modulus and the creep compliance respectively. ξ is a simple integration variable. Applying a Laplace transformation to [1.4] and [1.5] we obtain:

[1.6] $$\sigma(s) = sE(s)\varepsilon(s)$$

[1.7] $$\varepsilon(s) = sJ(s)\sigma(s)$$

With [1.6] and [1.7], we can link $E(t)$and $J(t)$:

[1.8] $$E(s) = \frac{1}{s^2 J(s)}$$

Considering a constant Poisson's ratio, the relation between the plane stress modulus and the Poisson's ratio is such as (Jones & Grasley, 2011) described:

[1.9] $$M(s) = \frac{E(s)}{1-\nu^2}$$

Moreover, plasticity occurring under a Berkovich tip is an important issue. To consider the effect of plasticity, (Vandamme et al., 2012) proposed the following relation,

[1.10] $$\dot{L}(t) = \frac{2a_U \dot{h}(t)}{P_{max}}$$

[1.11] $$\frac{M(t)}{M_0} = \frac{P(t)}{P_{max}}$$

where $L(t)$ is the contact creep compliance; $M(t)$ is the contact relaxation modulus; M_0 is the indentation modulus and a_U is the diameter of the contact area A_c. Thus, integrating both sides of equation [1.10], we have:

[1.12] $$L(t) - L(0) = \frac{2a_U}{P_{max}}\big(\mathrm{h(t)} - \mathrm{h(0)}\big) = \frac{2a_U}{P_{max}}\Delta\mathrm{h(t)}$$

The relation between $L(s)$ and $M(s)$ in the Laplace domain is:

[1.13] $$L(s) = \frac{1}{s^2 M(s)}$$

With [1.13], [1.8]and [1.9], $L(s)$ can be rewritten in as the function of $J(s)$, which leads to:

[1.14] $$L(s) = \frac{1-\nu^2}{s^2 E(s)} = (1-\nu^2)J(s)$$

Performing a Laplace inversion into the time domain, we get (Chen, Sorelli, Frech-Baronet, Sanahuja, & Vandamme, 2017):

[1.15] $$(1-\nu^2)\big(J(t)-J(0)\big) = \frac{2a_U}{P_{max}}\Delta \mathrm{h(t)}$$

where $\boldsymbol{J(0) = \frac{1}{E_0}}$ and $\boldsymbol{E_0}$ is the elastic modulus.

2.3.2 Logarithmic model

It is well established that multiple creeps in concrete follow a logarithmic function (Zdeněk P Bažant, Hauggaard, Baweja, & Ulm, 1997; Vandamme, 2008). Thus, the logarithmic creep compliance can be written as follow,

[1.16] $$J(t) - J(0) = \frac{1}{E_{v1}} \ln\left(1 + \frac{t}{\tau_1}\right)$$

where the modulus E_{v1} and the characteristic time τ_1 are fitting parameters. Applying a Laplace transformation we obtain,

[1.17] $$J(s) - \frac{J(0)}{s} = \frac{e^{s\tau_1} Ei(\tau_1)}{E_{v1} s}$$

where $Ei(x)$ is the exponential integral with the non-zero value of x given by:

[1.18] $$Ei(x) = \int_{-x}^{\infty} \frac{e^{-t}}{t} dt$$

From [1.8] and [1.17], the relaxation modulus reads as follows:

[1.19] $$E(s) = \frac{E_{v1}}{(J(0)E_{v1} + e^{s\tau_1} Ei(s\tau_1))s}$$

To solve [1.19], a numerical Laplace inversion is used, based on the following equations,

[1.20] $$f\left(t, \overline{M}\right) = \frac{\ln(2)}{(t)} \sum_{k=1}^{2\overline{M}} \varsigma_k f\left(\frac{k\ln(2)}{t}\right)$$

[1.21] $$\varsigma_k = (-1)^{\overline{M}+k} \sum_{j=[\frac{k+1}{2}]}^{k \wedge \overline{M}} \frac{j^{\overline{M}+1}}{\overline{M}!} \binom{\overline{M}}{j} \binom{2j}{j} \binom{j}{k-j}$$

where $\overline{M}$ is the positive integer that controls the precision of the inversed numerical function, $[\frac{k+1}{2}]$ is the greatest integer less than or equal to $\frac{k+1}{2}$ and $k \wedge \overline{M} = \min(k, \overline{M})$.

3 RESULTS AND ANALYSIS

3.1 Modulus and Hardness

Figure 4 presents typical 10 by 10 grid indentations, which were carried out on a bulk cement paste at 55% RH, with the corresponding mapping of indentation modulus *M* and hardness *H*. After testing, several indentation imprints were carefully observed with a digital microscope with a resolution of 0.1 μm. The result dispersion is quite limited, but a few heterogeneities are still visible (e.g., the few high values of *M* and *H* in μm may be explained by the presence of clinker particles in such indented volumes).

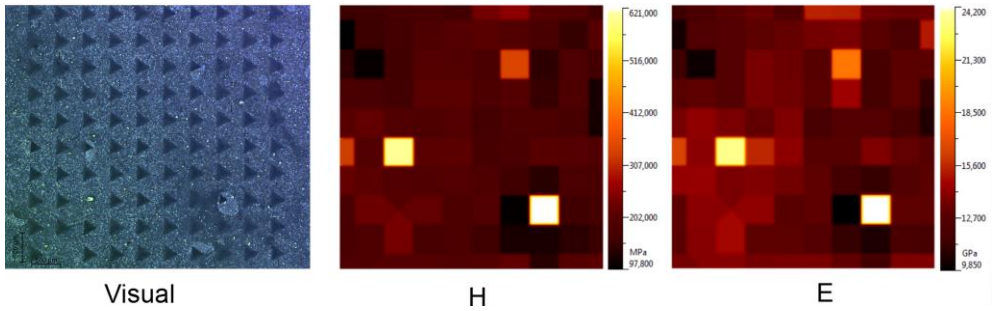

Figure 4: 10 by 10 indentations mapping in load control at 85% RH, with an inter-distance between imprints of 500 μm.

The mean values and the standard deviation (STD) for 100 tests of the indentation modulus *M* and hardness *H* for both force and displacement control tests at different RH are summarized in Table 2. As for the load control test, the indentation modulus *M* and hardness *H* were reduced of 6% and 27% by varying the equilibrium RH form 33% to 85%, respectively. The displacement control tests provided similar results: the indentation modulus *M* and hardness *H* were reduced of 4% and 22% by varying the equilibrium RH from 33% to 85%, respectively. Notably, previous works at a macroscopic scale showed a similar effect of RH on the Young's modulus and strength of concrete (Brooks, 2005; Wittmann, 1973). The strength increase at lower humidity level may be explained by a strengthening effect of the capillary forces in the desaturating pores (Dormieux, Sanahuja, & Maghous, 2006).

Table 2: Results of *M* and *H* for the microindentation tests in force/displacement control on the cement paste at the testing RH (mean $\pm$ STD).

	Force control $P_{max} = 8N$		**Displacement control** $h_{max} = 40\mu m$	
RH (%)	**Modulus (M_0) (MPa $\pm$ STD)**	**Hardness (H) ($GPa \pm STD$)**	**Modulus (M_0) (MPa $\pm$ STD)**	**Hardness (H) ($GPa \pm STD$)**
33	14.5$\pm$1.1	220$\pm$31	15.4$\pm$1.4	192$\pm$39
55	14.1$\pm$2.2	224$\pm$55	14.6$\pm$2.3	181$\pm$60
75	13.3$\pm$1.7	175$\pm$38	14.0$\pm$1.6	152$\pm$29
85	13.3$\pm$1.1	177$\pm$29	13.1$\pm$1.0	135$\pm$20

3.2 Creep compliance analysis

Figure 5 presents a comparison of the creep compliance modulus $J(t)$ obtained by microindentation testing at various RH levels for creep and relaxation testing. A total of 100 creep curves obtained by force control testing and 100 relaxation curves obtained by displacement control were averaged to performe a viscoelastoplastic analysis. The averaged creep curves (identified as C-RH) are fitted by the least square method, assuming the hypothesis that creep follows the logarithmic relation at equation [1.16]. The instantaneous deformation $J(0)$ is subtracted from the experimental value before fitting. From the averaged relaxation curves, the reciprocal creep curves (identify as R-RH) are fitted by the sum of square optimization, based on equation [1.19] and a numerical Laplace inversion (equation [1.20] and [1.21]). Table 3 presents the parameters calculated for each condition presented in Figure 5.

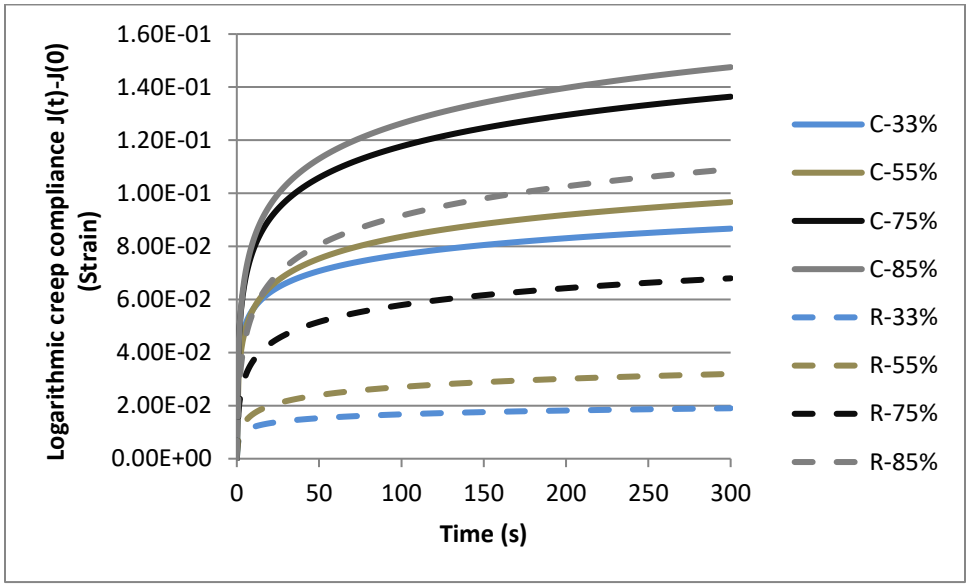

Figure 5: Comparison between creep compliance modulus $J(t)$ calculated from creep and relaxation experimental results for RH from 33% to 85%. Microindentation creep results, denoted by C-RH, are fitted by the least square method with the equation [1.16]. The microindentation relaxation results, named R-RH, are fitted by the sum of square optimization with the equation [1.19].

A clear augmentation of creep with RH humidity is observable as the E_{v1} decreases with the augmentation of RH. In the case of creep, from a linear regression a decrease of about 1.2 $MPa/\%RH$ of parameters E_{v1} is calculated with a determination coefficient $R^2 = 0.99$. In the case of relaxation, a decrease of about 8.0 $MPa/\%RH$ of parameters E_{v1} is calculated with a determination coefficient $R^2 = 0.96$.

Table 3: Logarithmic parameters calculated from creep and relaxation averaged curves.

	Creep Parameters				Relaxation Parameters			
Parameters	**C-33%**	**C-55%**	**C-75%**	**C-85%**	**R-33%**	**R-55%**	**R-75%**	**R-85%**
$E_{v1}(MPa)$	112.2	84.1	58.7	51.8	480.4	224.4	109.0	62.7
$\tau_1(s^{-1})$	0.018	0.088	0.100	0.144	0.033	0.232	0.182	0.322

A possible explanation can be attempted such as: a decrease of RH leads to a capillary suction increases and, by equilibrium, the disjoining pressure also increases quite instantaneously on the contact sites of C-S-H gels (Zdeněk P Bažant et al., 1997). The increase in the transversal compressive disjoining pressure may enhance internal friction of C-S-H sheets (Vandamme, Bažant, & Keten, 2015), reducing their sliding capacity and, thus, the long term creep.

3.3 Plastic analysis

As mentioned in section 2.3, plasticity cannot be separated from a microindentation force control test. During the holding phase, due to the viscoelastic nature of cement paste, the probe continues to penetrate the material in order to maintain a constant force for the whole duration of the test, generating plasticity in a continuous manner through time. On the other hand, during the holding phase of a displacement control test, no plasticity occurs. The probe is maintained at a specific depth and the force applied relaxed. Since no further deformation is imposed on the material, plasticity does not occur. Figure 6 presents the increase of the plastic deformation obtained from the difference between the creep compliance modulus obtained from the creep and relaxation modeling.

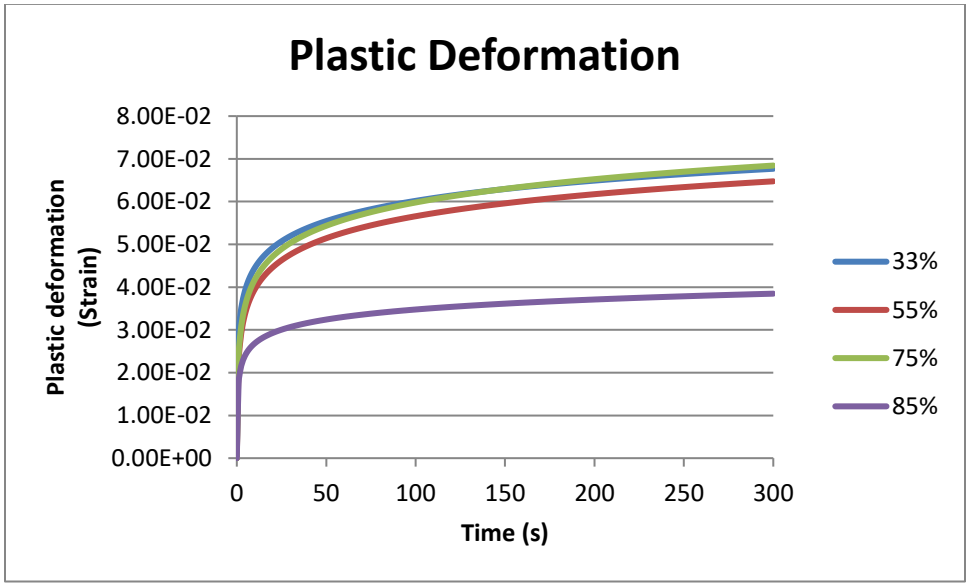

Figure 6: Comparison between plastic deformations for RH from 33% to 85%.

The plasticity of cement paste does not seem to be affected significantly by RH from 33% to 75% RH. At 85% however, a notable plasticity decrease can be observed. A possible explanation could be linked to a compaction of the C-S-H gel phenomenon. In force control, as the probe progress into the material, a stress is applied to the C-S-H gel causing water movement which lead to the reorganisation of the gel. Nonetheless, at 85% RH, the gel pore are not emptied and thus could limit the packing of the gel (Fleck, Otoyo, & Needleman, 1992; Jennings, 2004). Further investigation needs to be made in order to understand the mechanism at stake in plasticity of cement paste.

4 CONCLUDING REMARKS

This work presents a viscoelastoplastic analysis of creep and relaxation behaviour of cement paste by microindentation for different RH level from 33% to 85%. The presented results support the following conclusion:

1. an augmentation of the creep compliance function with RH for data obtained from force control and displacement control test, possibly linking to a change of the internal friction of the C-S-H sheets and

2. no noticeable variation of plasticity is observed form 33% to 75% RH. However, a noticeable reduction of plasticity at 85% RH suggests that the packing ability of the C-S-H gel is blocked by gel pores that are not emptied but filled with water.

5 ACKNOWLEDGEMENTS

The National Sciences and Engineering Research Council of Canada funding - Discovery Grant and the C.R.I.B. fellowship funding (No. 509437) are acknowledged here for supporting the present research and the scholarship of the first author.

6 REFERENCES

Bažant, Z. P., Hauggaard, A. B., Baweja, S., & Ulm, F.-J. (1997). Microprestress-solidification theory for concrete creep. I: Aging and drying effects. *Journal of Engineering Mechanics, 123*(11), 1188-1194.

Bažant, Z. P., Hubler, M. H., & Yu, Q. (2011). Excessive creep deflections: An awakening. *Concrete international, 33*(8), 44-46.

Benboudjema, F., Meftah, F., Sellier, A., Heinfling, G., & Torrenti, J. (2001). *A basic creep model for concrete subjected to multiaxial loads.* Paper presented at the Fourth International Conference on Fracture Mechanics of Concrete and Concrete Structures.

Brooks, J. (2005). 30-year creep and shrinkage of concrete. *Magazine of concrete research, 57*(9), 545-556.

Chen, Z., Sorelli, L., Frech-Baronet, J., Sanahuja, J., & Vandamme, M. (2017). Microindentation characterization and analytical modeling of the creep and relaxation behaviour of a cement paste at different relative humidity. *Manuscript submitted for publication.*

Christensen, R. (2012). *Theory of viscoelasticity: an introduction*: Elsevier.

Constantinides, G., Ravi Chandran, K. S., Ulm, F. J., & Van Vliet, K. J. (2006). Grid indentation analysis of composite microstructure and mechanics: Principles and validation. *Materials Science and Engineering: A, 430*(1–2), 189-202. doi:http://dx.doi.org/10.1016/j.msea.2006.05.125

Dormieux, L., Sanahuja, J., & Maghous, S. (2006). Influence of capillary effects on strength of non-saturated porous media. *Comptes Rendus Mécanique, 334*(1), 19-24.

Feldman, R. F. (1972). Mechanism of creep of hydrated Portland cement paste. *Cement and Concrete Research, 2*(5), 521-540.

Fischer-Cripps, A. C. (2000). *Introduction to contact mechanics*: Springer.

Fischer-Cripps, A. C. (2009). *The IBIS handbook of nanoindentation*: Fischer-Cripps Laboratories.

Fleck, N., Otoyo, H., & Needleman, A. (1992). Indentation of porous solids. *International journal of solids and structures, 29*(13), 1613-1636.

Jennings, H. M. (2004). Colloid model of C− S− H and implications to the problem of creep and shrinkage. *Materials and Structures, 37*(1), 59-70.

Jones, C. A., & Grasley, Z. C. (2011). Short-term creep of cement paste during nanoindentation. *Cement and Concrete Composites, 33*(1), 12-18.

Miller, M., Bobko, C., Vandamme, M., & Ulm, F.-J. (2008). Surface roughness criteria for cement paste nanoindentation. *Cement and Concrete Research, 38*(4), 467-476.

Neville, A., & Dilger, W. (1970). Creep of concrete: plain, reinforced, and prestressed.: Amsterdam, New York,: North-Holland Pub. Co. American Elsevier. xix.

Nguyen, D.-T., Alizadeh, R., Beaudoin, J. J., Pourbeik, P., & Raki, L. (2014). Microindentation creep of monophasic calcium–silicate–hydrates. *Cement and Concrete Composites, 48*, 118-126.

Tamtsia, B. T., & Beaudoin, J. J. (2000). Basic creep of hardened cement paste a re-examination of the role of water. *Cement and Concrete Research, 30*(9), 1465-1475.

Troxell, G., Raphael, J., & Davis, R. (1958). *Long-time creep and shrinkage tests of plain and reinforced concrete.* Paper presented at the ASTM Proceedings.

Ulm, F.-J., Vandamme, M., Bobko, C., Alberto Ortega, J., Tai, K., & Ortiz, C. (2007). Statistical Indentation Techniques for Hydrated Nanocomposites: Concrete, Bone, and Shale. *Journal of the American Ceramic Society, 90*(9), 2677-2692. doi:10.1111/j.1551-2916.2007.02012.x

Vandamme, M. (2008). *The nanogranular origin of concrete creep: a nanoindentation investigation of microstructure and fundamental properties of calcium-silicate-hydrates.* Massachusetts Institute of Technology.

Vandamme, M., Bažant, Z. P., & Keten, S. (2015). Creep of lubricated layered nano-porous solids and application to cementitious materials. *Journal of Nanomechanics and Micromechanics, 5*(4), 04015002.

Vandamme, M., Tweedie, C. A., Constantinides, G., Ulm, F.-J., & Van Vliet, K. J. (2012). Quantifying plasticity-independent creep compliance and relaxation of viscoelastoplastic materials under contact loading. *Journal of Materials Research, 27*(01), 302-312.

Wittmann, F. (1973). Interaction of hardened cement paste and water. *Journal of the American Ceramic Society, 56*(8), 409-415.

Zhang, Q. (2014). *Creep properties of cementitious materials: effect of water and microstructure: An approach by microindentation.* Université Paris-Est.